

Design of an improved high cooling power 4 K GM cryocooler and helium compressor

X H Hao

Advanced Research Systems, Inc.

7476 Industrial Parkway, Macungie, PA, 18062, USA

E-mail: xhao@arscryo.com.

Abstract. High cooling power 4 K cryocoolers are in high demand given their broad applications in such fields as magnetic resonance imaging (MRI) and low temperature superconductors. ARS has recently designed and developed a high cooling power 4 K pneumatic-drive GM cryocooler which achieves a typical cooling power of 1.75 W/4.2 K. Steady input power of our newly developed helium compressor supplied to the cold head is 11.8 kW at 60 Hz. The operational speed of the cold head is 30 RPM. The effects of geometries and operational conditions on the cooling performance of this 4 K GM cryocooler are also experimentally tested.

1. Introduction

With broad application of low temperature superconducting device, MRI, infrared detector and cryogenic electronics, the development of high cooling power 4 K cryocoolers are of critical importance. Since the 4 K two stage GM cryocooler was proposed and developed in the early 1990s by the application of rare-earth regenerator materials with high heat capacity around 4~12 K [1-2], a number of researches have been carried out to improve the cooling performance, stability, reliability and service life of 4 K GM cryocooler [3-8].

The conventional cooling power of the ARS pneumatic-drive GM cryocooler (DE210S) is 0.8 W at 4.2 K. In 2013, the cooling power of the DE210S was improved from 0.8 W to 1.1 W at 4.2 K by optimizing the regenerator materials and packing ratio inside the second stage displacer, as well as the operational conditions [9]. In 2014, the cooling power at 4.2 K was further improved from 1.1 W to 1.5 W (DE215S) by optimizing the displacer stroke and operational conditions [10]. Recently, a higher power helium compressor (ARS-20) was designed and developed by ARS. The cooling power of 1.75 W/4.2 K has been obtained in the cryocooler, while the steady input power of our newly developed helium compressor supplied to the cold head is 11.8 kW at 60 Hz. The effects of geometries and operational conditions on the cooling performance have been experimentally investigated in this paper.

2. Experimental set-up and procedures

The schematic diagram of the experimental setup and photo of the pneumatic-drive GM cryocooler (DE215S) are shown in Figure 1 and Figure 2, respectively. The pneumatic-drive GM cryocooler is different with mechanical-drive GM cryocooler in that it uses an internal pressure differential to move the displacer instead of a mechanical piston, which results in smaller vibrations.



The radiation heat loss of the second stage was reduced by the use of a radiation shield attached to the first stage cold station. The temperatures of the first stage and second stage were measured using calibrated silicon diode sensors. Two electrical heaters were installed on the cold stations to measure the cooling power. Two pressure transducers were installed in the inlet and exhaust of the cold head, respectively, so that the gas supply and return pressure can be measured.

The outer diameters of the first and second stage cylinders are $\text{\O}80$ mm and $\text{\O}38$ mm, while the lengths are 315 mm and 140 mm, respectively. The regenerator is placed inside the displacer. Copper screen and lead spheres were packed inside the first stage regenerator, while lead spheres and rare earth materials were packed inside the second stage regenerator.

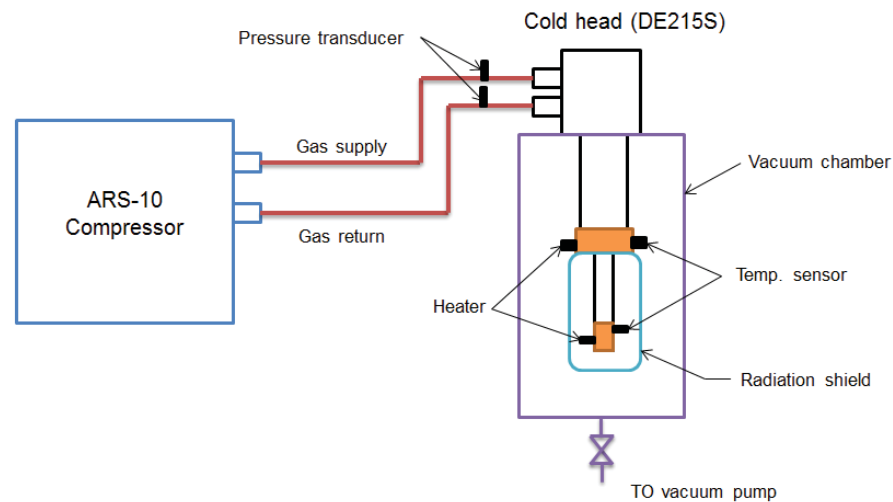


Figure 1. Schematic diagram of the experimental setup.



Figure 2. Photo of the pneumatic-drive GM cryocooler (DE215S).

3. Experimental results

3.1. Displacer stroke and operational speed

The effects of the displacer stroke and operational speed on the cooling performance of the second stage was experimentally investigated using strokes of 0.50'' (12.7 mm), 1.00'' (25.4 mm) and 1.25'' (31.8 mm). The corresponding expansion volumes of the second stage are 14.4 cm³, 28.8 cm³, and 35 cm³, respectively. The operational speed of the rotary valve was adjusted from 18 rpm to 60 rpm in the test. The system initial charge pressure was 1.60 MPa at an ambient temperature of 300 K. The cold head was driven by ARS-10 compressor.

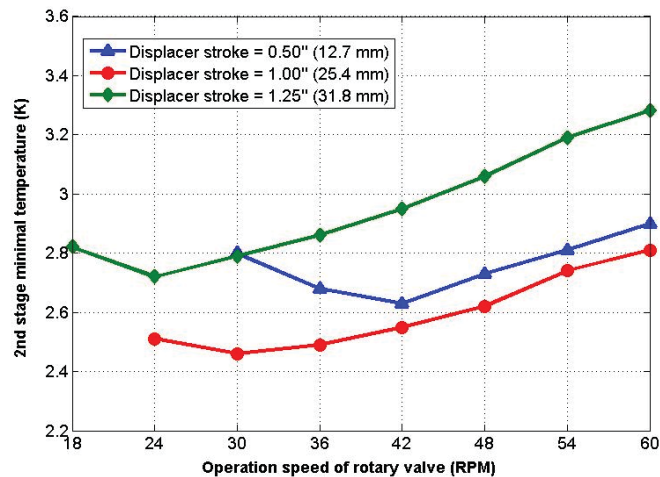


Figure 3. Plots of minimal temperatures of second stage as a function of operational speed.

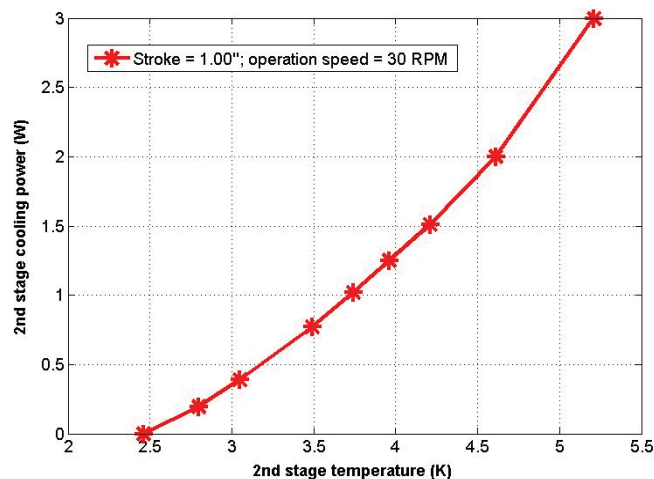


Figure 4. Plot of second stage cooling power as a function of temperature.

Figure 3 plots minimal temperatures of the second stage as a function of operational speed. It indicates that the minimum temperatures of the second stage with different strokes are all dependent on the operational speed. It also indicates that the operational speed at which the lowest minimal

temperature can be obtained becomes higher when the stroke is shorter. The optimal operational speeds corresponding to the displacer stroke of 0.50'', 1.00'' and 1.25'' are 42 rpm, 30 rpm and 24 rpm, respectively. The lowest minimal temperature of the second stage (2.46 K) is observed when the displacer stroke is 1.00'' and operational speed is 30 rpm. The author theorizes that the results came from the following: the expansion volume and PV work increases with the increasing displacer stroke, resulting in a considerable increase in the gross cooling power. However, this will also lead to an increase in the heat loss related with displacer stroke, such as shuttle loss. Therefore, there is an optimal displacer stroke for the cold head.

Figure 4 plots the second stage cooling power as a function of temperature when the stroke is 1.00'' and the operational speed is 30 rpm. A cooling power of 1.51 W at 4.21 K has been achieved, and the minimum temperature of the second stage is 2.46 K.

3.2. System initial charge pressure

The effect of the system initial charge pressure on the cooling performance of the cold head was experimentally investigated. The charge pressure was adjusted from 1.10 MPa to 1.70 MPa at a room temperature of 300 K. The operational speed of the rotary valve was kept at 30 rpm.

Figure 5 plots minimal temperatures of the cold head as a function of the system initial charge pressure. The cooling powers of the second stage at 4.20 K are plotted as a function of the charge pressure in Figure 6.

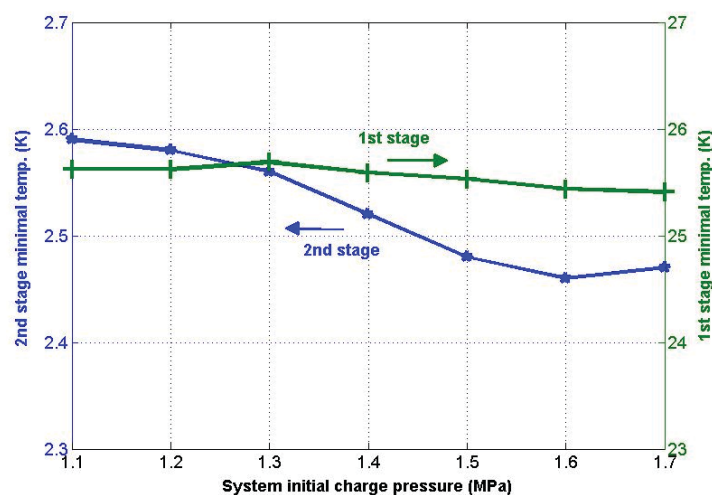


Figure 5. Plots of minimal temperatures of cold head as a function of charge pressure.

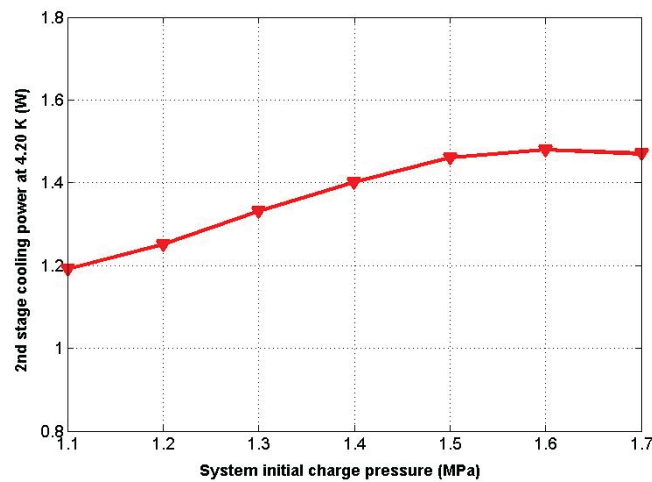


Figure 6. Plot of second stage cooling power at 4.20 K as a function of charge pressure.

The test results clearly indicate that the lowest minimal temperature of the second stage and maximum cooling power at 4.2 K are both observed when the system initial charge pressure is 1.60 MPa. The second stage minimal temperature decreases and then increases with increasing charge pressure. Its value varies between 2.46 K and 2.59 K. The first stage minimal temperature also varies with charge pressure. Its value varies between 25.4 K and 25.7 K. The minimal temperature is observed at 1.60~1.70 MPa. However, the first stage minimal temperature is not as sensitive as the second stage minimal temperature in the application. To have the lowest second stage temperature with maximum cooling power, it is preferable to set the charge pressure at 1.60 MPa for the DE215S.

3.3. Input power

The relationship between the compressor input power and the 4.2 K cooling power has also been investigated. In this test, the DE215S was driven by ARS-10 compressor and our newly developed helium compressor ARS-20. The outline drawings of ARS-10 and ARS-20 compressor are shown in Figure 7.

The main dimension of ARS-10 (W x L x H) is 19 x 21 x 26'' while the main dimension of ARS-20 (W x L x H) is 20.5 x 24.5 x 33.5''. The weights of the ARS-10 and ARS-20 are 250 lb. and 390 lb., respectively. The compressor motor input powers at 2.07 MPa / 0.69 MPa (discharge pressure / suction pressure) and 60 Hz are 7 kW and 12 kW, respectively.

In the test, the system initial charge pressure was kept at 1.60 MPa. The operational speed of the rotary valve was kept at 30 rpm.

The cooling powers of the second stage as a function of temperature are illustrated in Figure 8. From the above figure, it can be seen that the cooling powers of the second stage are evidently increased from 1.5 W to 1.75 W at 4.2 K. The power consumption at steady state (60 Hz) is 11.8 kW. The test results also indicate that the cooling power difference between two tests becomes larger as the temperature increases. However, the efficiency (COP) at 4.2 K decreases. The rate of increase of cooling power and COP at 4.2 K is not therefore proportional to the rate of increase of input power. Figure 9 plots the heat map of DE215S cold head driven by ARS-20 compressor.

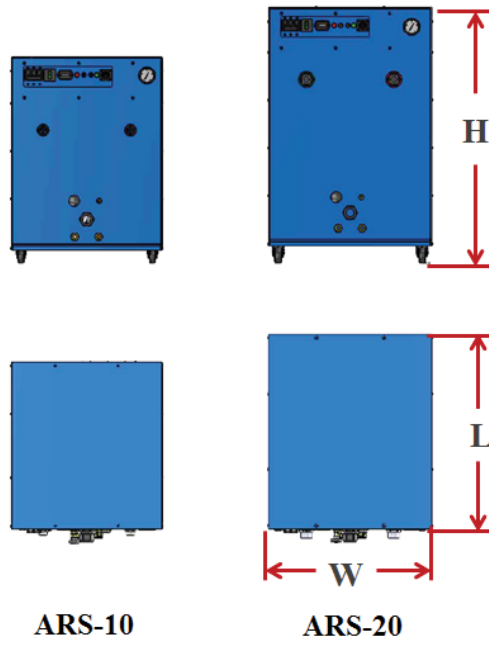


Figure 7. Outline drawings of ARS-10 and ARS-20 compressor.

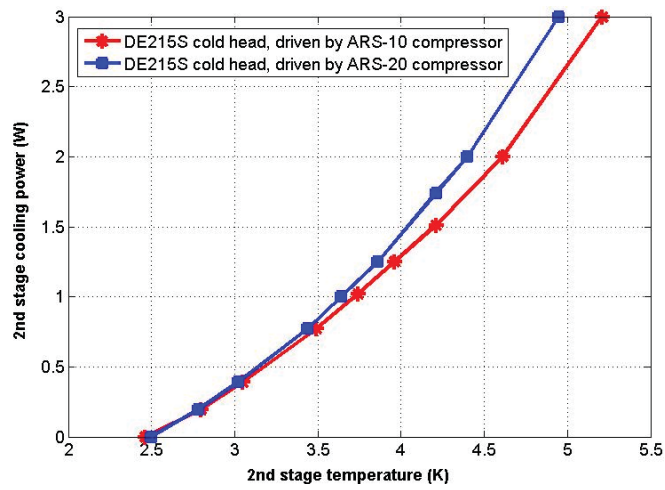


Figure 8. Plots of second stage cooling power as a function of temperature

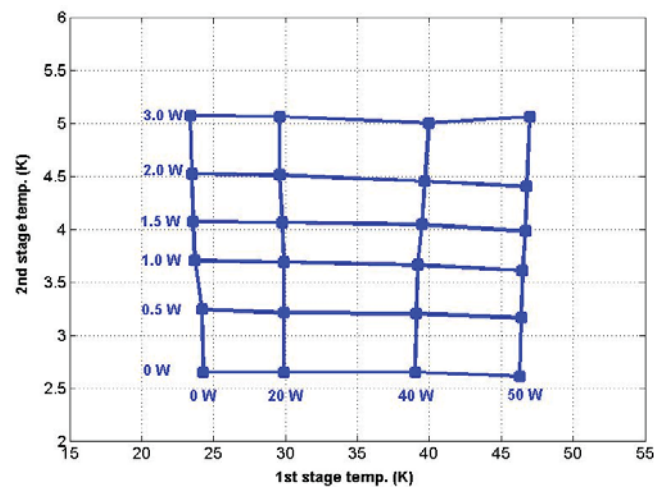


Figure 9. Heat map of DE215S (ARS-20 compressor)

4. Conclusions

A 1.5 W/4.2 K pneumatic-drive GM cryocooler has recently been designed and developed by ARS. A typical cooling performance of 1.50 W/4.2 K has been achieved driven by ARS-10 compressor. A maximal cooling power of 1.75 W/4.2 K has been achieved driven by new developed ARS-20 compressor in test runs; the power consumption at steady state (60 Hz) is 11.8 kW. The operational speed of the rotary valve is 30 rpm. The relationships between displacer stroke, operating conditions and the 4.2 K cooling power have also been experimentally tested. The test results indicate that the displacer stroke and operational speed are critical to the design of 4 K GM cryocooler.

5. References

- [1] Tokai Y 1989 *Proc. The 10th Intl. Workshop on Rare-Earth Magnets and their Application* Vol 1 (Society of Non-Traditional Technology)
- [2] Kuriyama T, Takahashi M, Nakagome H, Eda T, Seshake H and Hashimoto T 1992 *Japan. J. Appl. Phys.* **32** 1206
- [3] Morie T and Xu M Y 2012 *Cryocoolers 17* (Boulder: ICC Press) pp 247-252
- [4] Onish A, Li R, Asami H, Satoh T and Kanazawa Y 1997 *Proc. ICEC16/ICMC (Kitakyushu)* (Oxford, UK: Elsevier) p 351
- [5] Inaguchi T, Nagao M, Naka K and Yoshimura H 1997 *Proc. ICEC16/ICMC (Kitakyushu)* (Oxford, UK: Elsevier) p 335
- [6] Onish A, Li R, Satoh T and Kanazawa Y 1997 *Proc. ICEC16/ICMC (Kitakyushu)* (Oxford, UK: Elsevier) p 339
- [7] Usami T, Okamura T, Kabashima S, Ohtani Y, Hatakeyama H and Nakagome H 1999 *Cryocoolers 10* (New York: Kluwer Academic/Plenum Publishers) pp 587-592
- [8] Inaguchi T, Nagao M, Naka K and Yoshimura 1999 *Cryocoolers 10* (New York: Kluwer Academic/Plenum Publishers) pp 593-602
- [9] Hao X H and Yao S H 2014 *Advances in Cryogenic Engineering* (Melville: AIP Publishing LLC) pp 1157-1161
- [10] Hao X H, Yao S H and Schilling T 2015 Design and experimental investigation of the high efficiency 1.5W/4.2K pneumatic-drive GM cryocooler *Cryogenics*. **70** 28